High Accumulation of 2-Deoxy-2-Fluorine-18-Fluoro-D-Galactose by Well-Differentiated Hepatomas of Mice and Rats

Hiroshi Fukuda, Jutaro Takahashi, Takehiko Fujiwara, Keiichirou Yamaguchi, Yoshinao Abe, Kazuo Kubota, Tachio Sato, Hidemitsu Miyazawa, Jun Hatazawa, Masao Tada, Kiichi Ishiwata and Tatsuo Ido

Department of Radiology and Nuclear Medicine and Department of Pharmacology, The Research Institute for Tuberculosis and Cancer, Tohoku University, Sendai, Japan, The Cyclotron and Radioisotope Center, Tohoku University, Sendai, Japan

The potential application of 2-deoxy-2-[^{18}F]fluoro-D-galactose for the detection and evaluation of hepatomas with PET was examined in mouse and rat liver tumor models. Biodistribution studies showed that uptake of this marker was high in well-differentiated, spontaneous hepatoma of C3H mice at almost 92% of the normal liver level. The uptake by well-differentiated Morris rat hepatoma (5123D) was relatively high and second to that of the C3H hepatoma. On the other hand, uptake values for poorly differentiated mouse hepatoma (MH129P), rat hepatomas (AH109A, AH272), mouse melanoma (B-16) and mammary carcinoma (FM3A) were very low and only 14%–18% of that in the normal liver. The results suggest that while well-differentiated hepatomas maintain a high galactose metabolic activity, poorly differentiated hepatomas or other tumors lose this to a large extent. Consequently, this radiopharmaceutical can be used with PET for biochemical characterization of hepatomas and the differential diagnosis between hepatomas and other cancers.

J Nucl Med 1993; 34:780–786

Increased glycolysis is one of the most important characteristics of cancer cells. Extensive studies on the glucose metabolism of experimental hepatomas were reported in the 1960s by Weber (*1*) and Burk et al. (*2*), showing an increase in glycolytic enzymes and a decrease in gluconeogenetic enzymes in relation to increase in tumor growth rates. More recently, 2-deoxy-2-[^{18}F]fluoro-D-glucose (^{18}FDG), a positron labeled glucose analog, has been proposed as a good tracer for in vivo cancer detection and evaluation (*3,4*). Fluorine-18-FDG with PET has been used to grade gliomas (*5*). Glucose consumption measured in this way was found to correlate well with the prognosis of gliomas (*6*) and meningiomas (*7*). This marker has also been used to image liver tumors (*8,9*). These previous studies focused on evaluating the viability of cancer cells, which is an essential and nonspecific factor independent of cancer type.

However, cancer cells occasionally express the phenotypes of their original tissues and organs and the degree of this expression may represent the degree of differentiation. There thus arises the possibility to use a radiolabeled tracer, which is a substrate for a specific enzyme, a ligand of a specific receptor or a monoclonal antibody to a specific tissue to assess cancers originating from a specific tissue. The origin of the tumor should be detectable so that the degree of phenotype expression, that is the degree of differentiation of the cancer, could be evaluated. For example, iodine is a source for thyroid hormone synthesis and radioiodine accumulates in some types of thyroid cancers. Iodine-131-meta-iodobenzylguanidine (MIBG) has been developed for adrenal imaging (*10*) and also accumulates in pheochromocytomas (*11*) originating from the adrenal medulla. Such a means of tumor characterization with PET may allow other avenues for cancer diagnosis.

We have developed a positron labeled galactose analog, 2-deoxy-2-[^{18}F]fluoro-D-galactose (^{18}FDGal) to evaluate regional galactose metabolism in the liver using PET (*12–19*). It is phosphorylated by galacto-kinase and then trapped after the second metabolic step of the galactose pathway (*18*). In tissues, the most pronounced activity of these enzymes is found in the liver and can therefore be considered as a liver-specific tracer and a new probe for the evaluation of galactose metabolism in this organ using PET (*13,17*). In a preliminary PET study, we also found that ^{18}FDGal accumulates in hepatocellular carcinomas (HCCs) that originate from hepatocytes but not in metastatic liver tumors of other origins (*20–21*). In order to investigate the mechanisms underlying high specific accumulation of ^{18}FDGal in HCC, we examined its uptake with well-differentiated, spontaneous hepatoma of C3H

Received June 10, 1992; revision accepted Jan. 18, 1993.

For correspondence and reprints contact: Hiroshi Fukuda, MD, Department of Radiology and Nuclear Medicine, The Research Institute for Tuberculosis and Cancer, Tohoku University, 4-1 Seiryo-machi Aoba-ku, Sendai 980, Japan.

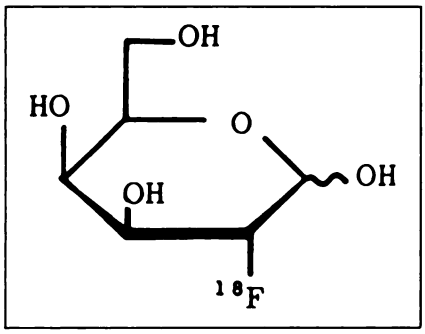

FIGURE 1. Chemical structure of ^{18}FDGal.

mice and well-differentiated Morris hepatoma of the Buffalo rat and compared the values with those for poorly differentiated hepatomas and tumors other than liver cancers.

MATERIALS AND METHODS

Preparation of ^{18}FDGal

Galactose was synthesized by the reaction of tri-O-acetyl-D-galactal with [^{18}F]CH3COOF, as previously described (*12,15*). Figure 1 shows the chemical structure of the compound. The radiochemical purity of the compound as determined by high-performance liquid chromatography (HPLC) was more than 99%, and its specific radioactivity was in the range of 47–80 MBq/μmole at the end of synthesis and 34–68 MBq/μmole at the time of administration to the animals.

Animals and Tumors

Spontaneous hepatoma of C3H mice (C3H/HeMs) and an ascitic hepatoma of mice (C3H/HeNCrj), MH129P, was used as mice hepatoma models for the biodistribution study. Since the incidence of spontaneous hepatoma increases with age, reaching 70%–80% at 15 mo of age, at which time the tumors grow slowly and are well-differentiated in histology (*22*), experiments were performed with mice aged 15 to 17 mo that weighted from 35 to 42 g. Because MH129P tumors grow rapidly and are poorly differentiated histologically (*23*), the MH129P cells, ascitic tumor cells maintained by serial intraperitoneal injection, were inoculated subcutaneously into the back of male C3H mice. The experiments were performed when the tumors were 5–10 mm in diameter.

Morris hepatoma of the Buffalo rat, 5123D, and two Donryu rat ascitic hepatomas, AH109A and AH272, were also utilized for the biodistribution studies. 5123D is a minimum-deviated hepatoma, which grows slowly and is moderately differentiated in histology (*24*). AH109A and AH272 lines grow rapidly and are poorly differentiated in histology (*25,26*). Cell suspensions of 5123D were prepared from excised tumors and inoculated subcutaneously into the back of male Buffalo rats (weighing 100–120 g). AH109A and AH272 ascitic tumor cells were also inoculated subcutaneously into the backs of male Donryu rats (weighing 120–140 g). The experiments were performed when the tumors were greater than 10 mm in diameter. Body weights ranged from 140 to 180 g for Buffalo rats and 160 to 200 g for Donryu rats. For tumors other than hepatomas, a mammary carcinoma of C3H mice (FM3A) and a melanoma of C57BL mice (B-16) were also used.

Biodistribution Study

Fluorine-18-FDGal (370 KBq in 0.2 ml isotonic saline) was injected into each mouse or rat through the lateral tail vein. The animals were killed by neck dislocation at predetermined times after injection and tissues and tumors were removed, blotted and weighed. Radioactivity was counted in a NaI automated counter, decay-corrected and expressed as the percentage of the injected dose per gram of tissue (%ID/g) or the differential absorption ratio (DAR), which is the %ID/g normalized by animal body weight. Four to seven animals were used for each data point.

Autoradiography

Autoradiograms of hepatoma bearing C3H mice were made after injection of 22 MBq of ^{18}FDGal. The mice were killed by chloroform at 30 min after injection, coated with 4% carboxymethylcellulose (CMC), frozen in dry ice and acetone (−80°C), mounted in 4% CMC and refrozen at −80°C. Sections (40 μm in thickness) were cut from frozen blocks using an auto-cryotome and placed in contact with film for ^{3}H (Sakura Co. Ltd) precooled at −20°C. The films were exposed in a freezer (−20°C) for 6–12 hr and then developed.

Autoradiograms of 5123D bearing Buffalo and AH109A bearing Donryu rats were also made after injection of 74 MBq of ^{18}FDGal using the same methods mentioned above.

RESULTS

Table 1 shows the biodistribution and tumor-to-tissue ratios in spontaneous hepatoma-bearing C3H mice. The accumulation of ^{18}FDGal in normal liver rapidly increased with time and reached a near plateau by 10 min. The value at 60 min was 20.1 %ID/g. Tumor uptake was also high and gradually increased with time. The value was 18.4 %ID/g at 60 min, with 92% of that in the liver. Radioactivity in the other organs was low except for the kidney which was 14.6 %ID/g, with 73% of that in the liver. Tumor-to-tissue ratios at 60 min were high for blood (12.7), muscle (24.2) and all the other organs except the liver (0.92) and kidney (1.25).

Table 2 shows the biodistribution of ^{18}FDGal and tumor-to-tissue ratios in 5123D hepatoma-bearing rats. Liver uptake reached a near plateau by 10 min and the value was 7.90 %ID/g at 60 min after the injection. Radioactivity in the other organs was low except for the kidney, which had a value of 4.10 %ID/g at 60 min, with 52% of that in the liver. Tumor uptake gradually increased with time for a value of 2.58 %ID/g at 60 min. The tumor-to-liver ratio at 60 min was 0.33, which was relatively high but lower than that in spontaneous C3H hepatoma studies (0.92). The tumor-to-blood and muscle ratios at 60 min postinjection were very high at 9.56 and 9.92, respectively.

Table 3 shows the biodistribution of ^{18}FDGal and tumor-to-tissue ratios in AH109A hepatoma-bearing rats. Liver uptake reached a near plateau at 30 min for a value of 8.54 %ID/g at 60 min postinjection. Radioactivity in the other organs was low except for the kidney, which was 2.81 %ID/g at 60 min, with 33% of that in the liver. Tumor uptake was low, although it gradually increased with time

TABLE 1
Fluorine-18 Radioactivity Following Injection of ^{18}FDGal in Spontaneous Hepatoma-Bearing C3H Mice

Organ	Uptake (%dose/g)*			
	2 min	10 min	30 min	60 min
Tumor	10.1 ± 1.74	11.9 ± 2.17	14.1 ± 6.83	18.4 ± 3.14
Blood	3.92 ± 1.02	2.15 ± 0.65	1.48 ± 0.36	1.45 ± 0.15
	(2.59)†	(5.50)	(9.50)	(12.7)
Heart	4.97 ± 0.98	3.93 ± 1.03	3.09 ± 0.52	3.13 ± 0.99
	(2.04)	(3.02)	(4.56)	(5.90)
Liver	10.2 ± 2.90	18.1 ± 2.63	18.0 ± 4.78	20.1 ± 2.79
	(1.01)	(0.66)	(0.78)	(0.92)
Kidney	13.3 ± 2.73	12.7 ± 3.78	13.3 ± 2.21	14.6 ± 2.04
	(0.76)	(0.93)	(1.36)	(1.26)
Small intestine	5.33 ± 2.06	6.03 ± 1.23	5.67 ± 1.59	6.07 ± 0.91
	(1.89)	(1.97)	(2.49)	(3.03)
Brain	2.13 ± 0.35	2.24 ± 0.55	2.18 ± 1.47	2.83 ± 0.30
	(4.76)	(5.29)	(6.46)	(6.51)
Muscle	1.65 ± 0.27	0.95 ± 0.29	0.91 ± 0.32	0.76 ± 0.30
	(6.15)	(12.5)	(15.5)	(24.2)

*Mean value obtained from five to seven mice ±s.d.
†Tumor-to-tissue ratio.

and reached a near plateau at 60 min with a value of 1.37 %ID/g. The tumor-to-liver ratio at 60 min was 0.16 which was much lower than that for spontaneous C3H hepatomas (0.92). Tumor-to-blood and muscle ratios 60 min postinjection were very high at 5.27 and 13.7, respectively.

Table 4 shows the tumor uptake data and tumor-to-liver ratios at 60 min for the various tumors examined in the present experiments. The tumor uptakes are expressed as DAR in addition to %dose/g in order to normalize the big difference in body weight between mice and rats. For liver uptake expressed in this way, the values ranged from 8 to 14, the difference in value between mice and rats being smaller than that based on %dose/g data.

Among the tumors, uptake by spontaneous C3H hepatomas was the highest (6.86 by DAR) followed by that of 5123D (3.50 by DAR), while the poorly differentiated mouse and rat hepatomas demonstrated very low values. The uptakes were 1.30, 1.75 and 1.86 for MH129P, AH109A and AH272, respectively. Uptakes by tumors other than hepatomas were very low, the values being 1.40 and 1.13 for FM3A and B-16, respectively. The tumor-to-liver ratio was also extremely high for the spon-

TABLE 2
Fluorine-18 Radioactivity Following Injection of ^{18}FDGal in Morris Rat Hepatoma (5123D)

Organ	Uptake (%dose/g)*			
	2 min	10 min	30 min	60 min
5123D	1.52 ± 0.44	2.38 ± 0.06	2.31 ± 0.63	2.58 ± 0.40
Blood	1.14 ± 0.20	0.68 ± 0.02	0.28 ± 0.05	0.27 ± 0.02
	(1.33)†	(3.50)	(8.25)	(9.56)
Heart	0.70 ± 0.10	0.72 ± 0.08	0.48 ± 0.07	0.52 ± 0.07
	(2.17)	(3.31)	(4.81)	(4.96)
Liver	3.53 ± 0.97	6.90 ± 0.46	7.23 ± 0.69	7.90 ± 0.74
	(0.43)	(0.34)	(0.32)	(0.33)
Kidney	3.47 ± 0.74	4.01 ± 0.62	3.54 ± 0.89	4.10 ± 0.50
	(0.44)	(0.59)	(0.65)	(0.63)
Small intestine	1.00 ± 0.27	1.31 ± 0.27	0.93 ± 0.28	1.33 ± 0.36
	(1.52)	(1.82)	(2.48)	(1.94)
Brain	0.54 ± 0.05	0.69 ± 0.06	0.64 ± 0.08	0.78 ± 0.07
	(2.81)	(3.45)	(3.61)	(3.31)
Muscle	0.33 ± 0.09	0.25 ± 0.04	0.20 ± 0.08	0.26 ± 0.07
	(4.60)	(9.52)	(11.6)	(9.92)

*Mean value obtained from six rats ±s.d.
†Tumor-to-tissue ratio.

TABLE 3
Fluorine-18 Radioactivity Following Injection of ^{18}FDGal in Hepatoma-Bearing (AH109A) Rats

Organ	Uptake (%dose/g)*			
	10 min	30 min	60 min	120 min
AH109A	0.89 ± 0.19	1.08 ± 0.26	1.37 ± 0.17	1.41 ± 0.13
Blood	0.53 ± 0.04	0.29 ± 0.02	0.26 ± 0.04	0.24 ± 0.02
	(1.68)†	(3.72)	(5.27)	(5.88)
Heart	0.63 ± 0.03	0.34 ± 0.03	0.34 ± 0.04	0.34 ± 0.05
	(1.41)	(3.18)	(4.03)	(4.15)
Liver	5.60 ± 0.39	8.00 ± 0.68	8.54 ± 0.84	7.96 ± 0.42
	(0.16)	(0.14)	(0.16)	(0.18)
Kidney	3.10 ± 0.34	3.10 ± 0.26	2.81 ± 0.36	2.49 ± 0.19
	(0.29)	(0.35)	(0.49)	(0.57)
Small intestine	0.78 ± 0.06	0.80 ± 0.11	0.71 ± 0.10	0.87 ± 0.11
	(1.14)	(1.35)	(1.93)	(1.62)
Brain	0.56 ± 0.03	0.66 ± 0.06	0.68 ± 0.07	0.72 ± 0.04
	(1.59)	(1.64)	(2.01)	(1.96)
Muscle	0.18 ± 0.01	0.11 ± 0.02	0.10 ± 0.02	0.10 ± 0.03
	(4.94)	(9.82)	(13.7)	(14.1)

*Mean value obtained from six rats ±s.d.
†Tumor-to-tissue ratio.

taneous C3H hepatoma (0.92), relatively high for 5123D (0.46) and much lower (range 0.14 to 0.18) for other tumors.

Figures 2, 3 and 4 illustrate ^{18}FDGal autoradiograms for a spontaneous C3H hepatoma-bearing mouse, a 5123D hepatoma-bearing rat and an AH109A hepatoma-bearing rat, respectively. Very high radioactivities are apparent in the liver of the C3H mouse, the Buffalo rat and the Donryu rat (arrows). Radioactivity in the spontaneous C3H hepatoma (Fig. 2B) was similarly very high and almost the same as that in the liver (Fig. 2A). Radioactivity in the 5123D tumor case was also high but lower than in the liver (Fig. 3). In contrast, the AH109A tumor showed very low radioactivity when compared to the liver, but it was still clearly visualized from the surrounding soft tissues (Fig. 4).

TABLE 4
Tumor Uptake and Tumor-to-Liver Ratios of ^{18}FDGal in Various Tumors

Tumor	Animal	Uptake at 60 min* (%dose/g)	DAR†	Tumor/Liver
HCC	C3H	18.4 ± 3.14	6.86 ± 1.18	0.92
MH129P	C3H	5.77 ± 1.87	1.37 ± 0.50	0.17
FM3A	C3H	6.37 ± 0.50	1.40 ± 0.09	0.18
B-16	C57BL	4.53 ± 0.83	1.13 ± 0.17	0.14
5123D	Buffalo	2.58 ± 0.40	3.53 ± 0.74	0.33
AH272	Donryu	1.51 ± 0.20	1.86 ± 0.21	0.18
AH109A	Donryu	1.37 ± 0.20	1.75 ± 0.12	0.16
Liver				
	C3H‡	20.1 ± 2.79	7.99 ± 1.47	
	C3H§	35.2 ± 4.10	8.80 ± 0.88	
	C57BL	32.7 ± 2.40	8.18 ± 0.80	
	Buffalo	7.90 ± 0.74	10.8 ± 1.26	
	Donryu	8.54 ± 0.84	13.8 ± 1.40	

*Mean value obtained from four to seven animals ±s.d.
†DAR = Tissue activity (cpm/g)/Injected dose (cpm)/body weight (g).
‡Fifteen to 17-mo old (body weight, 35–43 g).
§Ten-week-old (body weight, 27–32 g).

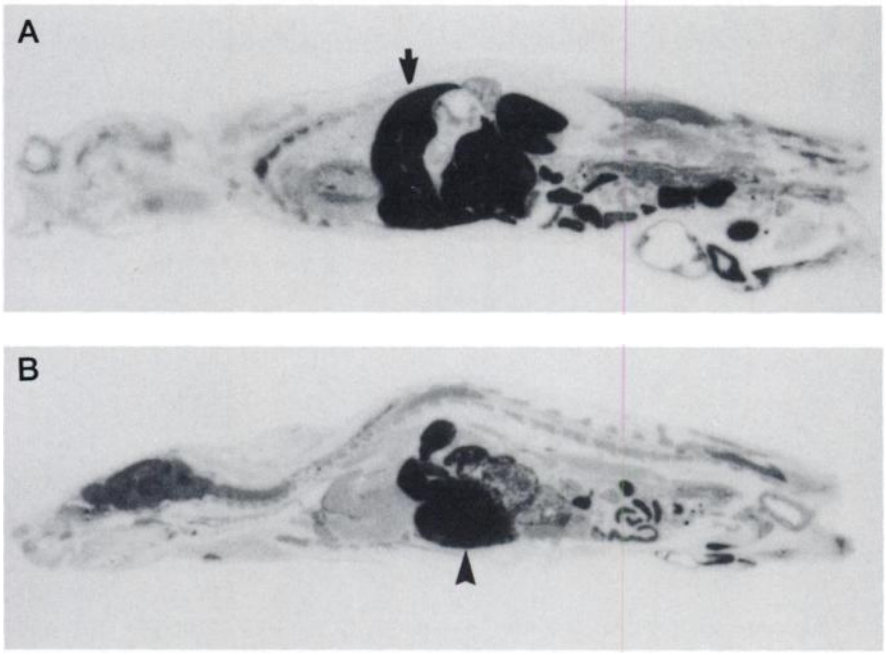

FIGURE 2. Autoradiograms of a spontaneous hepatoma-bearing C3H mouse 30 min after injection of ^{18}FDGal. (A) A section where only normal liver (arrow) is seen. (B) Another section from the same mouse where the spontaneous hepatoma (arrow head) was seen.

DISCUSSION

D-galactose is phosphorylated, after active membrane transport, to galactose-1-phosphate by galactokinase, catalyzed through further steps of the metabolic pathway and is finally used for glycoprotein synthesis or changed to glucose to be used as an energy source. Enzymes from galactose metabolism occur in almost all tissues, but the liver has the highest activity (*27*) and its ability to eliminate galactose is an important indicator of liver function (*28,29*).

We earlier reported that ^{18}FDGal is taken up by the liver in a competitive process with D-galactose (*13*), phosphorylated by galactokinase in the same way and then trapped after a second uridylation step of the galactose pathway (*18*). Consequently, uptake of ^{18}FDGal directly reflects galactose metabolic activity in the tissue. Biodistribution studies revealed the highest radioactivity of ^{18}FDGal among normal tissues in the liver, while a relatively high activity was also found in the kidney. The other organs demonstrated only low uptake. The ranked order of uptake (liver > kidney > intestine > brain > muscle) is consistent with the order of galactokinase activity (*27*).

We also reported earlier that ^{18}FDGal is taken up into various animal tumors, including poorly differentiated hepatomas, through phosphate and urydilate trapping as in the liver (*19*). The incorporation by hepatomas was slightly higher than in other tumors. In the present study, accumulation of ^{18}FDGal was particularly high in spontaneous hepatoma of C3H mice and also relatively high in the 5123D Morris hepatoma in contrast to the low levels observed for poorly differentiated hepatomas (MH129P, AH109A, AH272) and other tumors (FM3A, B-16). Autoradiography confirmed these results.

Differences in ^{18}FDGal uptake were observed between spontaneous C3H hepatoma and 5123D Morris hepatoma, although both are considered to be well-differentiated tumor models. Histological examination, however, revealed that the spontaneous mouse hepatoma was highly differentiated and deviated slightly from normal liver, while Morris hepatoma was only moderately differentiated. The growth rate of C3H hepatomas cannot be easily evaluated because the tumors occur spontaneously in the liver, but the mice survived for several months even after development of palpable lesions. This is at least indicative of extremely slow growth, whereas the measurable increase in size of 5123D transplants was appreciable, although slower than that of AH109A or AH272. This may be the reason for the relatively high uptake of ^{18}FDGal in C3H hepatomas, although galactose

FIGURE 3. An autoradiogram of a 5123D Morris hepatoma-bearing Buffalo rat 30 min after injection of ^{18}FDGal. Normal liver (arrow) demonstrates the highest activity among the tissues, while the 5123D tumor (arrow head) is lower in the liver but is still relatively high.

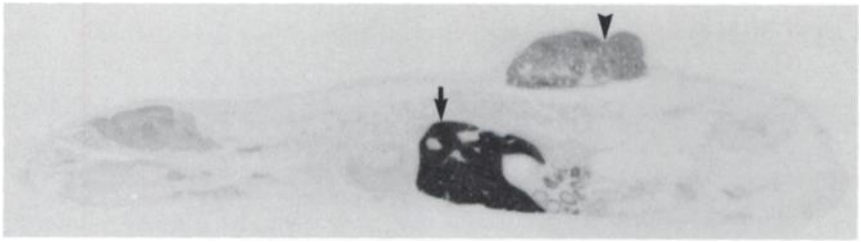

FIGURE 4. An autoradiogram of an AH109A hepatoma-bearing Donryu rat 30 min after injection of ^{18}FDGal. Liver activity (arrow) is high, while that in the tumor is low. However, the tumor can be clearly delineated due to lack of radioactivity in the surrounding soft tissues.

metabolic activity is not the only factor determining tumor differentiation and growth kinetics.

A species difference in galactose metabolism between mice and rats might also be considered as a contributory factor. The possibility of size variation was assessed by use of DAR values, which represent relative uptake normalized for body weight, and the normal mouse liver was found to have a lower rate than that of rats. Furthermore, uptake in a poorly differentiated mouse hepatoma (MH129P) was as low as that in poorly differentiated rat hepatomas (AH109A, AH272), indicating that high uptake by spontaneous hepatomas was not simply due to high galactokinase activity in mouse tissue.

Bauer et al. (*30*), in examining changes in galactose metabolism between experimental hepatomas and normal liver, found a decrease in galactose uptake and an increase in UDP-galactose 4′-epimerase, depending on tumor growth rate. These data suggest that well-differentiated hepatomas maintain galactose metabolic enzymes, but these are lost when the tumor becomes more malignant. Their report is in line with our present data for ^{18}FDGal uptake and is similar to our preliminary clinical PET study, which showed high ^{18}FDGal accumulation in HCCs originating from hepatocytes and very low accumulation in metastatic liver cancers (*20,21*).

For tumor imaging, ^{18}FDGal is a good tracer for the detection of metastases from HCCs. In the case of C3H hepatoma, the tumor-to-blood and tumor-to-muscle ratios were 12.7 and 24.3 at 60 min, respectively. For the poorly differentiated hepatoma (AH109A), the ratio was 5.27 and 13.7, respectively. The latter compares favorably with previously reported values of tumor-to-muscle ratios obtained for ^{18}F-fluoro-deoxyglucose (6.46 at 60 min) (*4*), ^{18}F-fluorodeoxy-uridine (8.80 at 60 min) (*31*) and ^{11}C-methionine (4.70 at 20 min) (*32*) using the same tumor line (AH109A). From this very high tumor-to-muscle ratio, we may obtain a good image of hepatoma metastases located in sites other than the liver and kidney. Autoradiography confirmed that the AH109A tumor inoculated into the back of the rat could be clearly delineated from the surrounding soft tissues.

Fluorine-18-FDG is widely used for the detection and evaluation of brain and lung tumors and can also be used for imaging liver cancers from background parenchyma. We have shown on autoradiographs that ^{18}FDG could positively delineate hepatomas that had been inoculated in the liver (*4*). This was achieved by a combination of high ^{18}FDG uptake in tumor tissue and rapid clearance from normal liver. Consequently, ^{18}FDG is more useful than ^{18}FDGal in detecting hepatomas because ^{18}FDGal uptake in normal liver is even higher than that in well-differentiated hepatomas and the lesions in the liver will always be negatively delineated. However, ^{18}FDGal is advantageous in that its uptake by HCCs is far higher than the uptake in metastatic liver cancers (*20,21*).

In conclusion, ^{18}FDGal uptake can be utilized to assess galactose metabolism in tumors, and PET studies using this marker can be employed for the detection and biochemical characterization of HCCs and for the differential diagnosis between HCC and metastatic liver cancers. We also sought to devise a method for in vivo characterization of HCCs using ^{18}FDGal as an indicator of galactose metabolic activity. However, since uptake on PET images does not directly represent enzyme activity, but rather is the result of interaction between many factors, such as tumor metabolism, blood flow, blood volume and fraction of necroses, mathematical modeling is necessary for quantitative analysis. This could be done using three- or four-compartment analyses based on metabolic studies (*19*). Additionally, clinical PET investigations should be combined with tumor pathology, biochemistry and patient prognosis.

ACKNOWLEDGMENTS

This study was supported by a grant-in-aid for cancer research from the Japanese Ministry of Health and Welfare (nos. 1-40 and 3-35) and from the Ministry of Education, Science and Culture (no. 02151072). The authors are very grateful to the staff of CYRIC, Tohoku University for the use of the cyclotron and thank Prof. M. Watanabe for providing the 5123D hepatomas and Mr. Y. Sugawara, Mrs. R. Kubota and Mr. K. Kikuchi for technical assistance.

REFERENCES

1. Weber G, Morris HP. Comparative biochemistry of hepatomas. III. Carbohydrate enzymes in liver tumors of different growth rate. *Cancer Res* 1963;23:987–993.
2. Burk D, Wood M, Hunter J. On the significance of glycolysis for cancer growth with special reference to Morris rat hepatomas. *J Natl Cancer Inst* 1967;38:839–863.
3. Som P, Atkins HL, Bandoypadhyay D, et al. A fluorinated glucose analog, 2-fluoro-2-deoxy-D-glucose (F-18): nontoxic tracer for rapid tumor detection. *J Nucl Med* 1980;21:670–675.
4. Fukuda H, Matsuzawa T, Abe Y, et al. Experimental study for cancer diagnosis with positron-labeled fluorinated glucose analogs: [^{18}F]-2-fluoro-2-deoxy-D-mannose: a new tracer for cancer detection. *Eur J Nucl Med* 1982;7:294–297.

5. Di Chiro G, DeLaPaz RL, Brooks RA, et al. Glucose utilization of cerebral gliomas measured by [^{18}F]fluorodeoxy glucose and positron emission tomography. *Neurology* 1982;32:1323–1329.
6. Pantronas NJ, Di Chiro G, Kufta C, et al. Prediction of survival in glioma patients by means of positron emission tomography. *J Neurosurg* 1985; 62:816–822.
7. Di Chiro G, Hatazawa J, Katz DA, Rizzoli HV, De Michele DJ. Glucose utilization by intracranial menigiomas as an index of tumor aggressivity and probability of recurrence: a PET study. *Radiology* 1987;164:521–526.
8. Yonekura Y, Benau RS, Brill AB, et al. Increased accumulation of 2-deoxy-2-[^{18}F]fluoro-D-glucose in liver metastases from colon carcinoma. *J Nucl Med* 1982;23:1133–1137.
9. Fukuda H, Matsuzawa T, Itoh M, Abe Y, Yoshioka S, Yamada K. Experimental and clinical study of cancer diagnosis with (F-18) FDG using positron emission tomography [Abstract]. *J Nucl Med* 1984;25:50.
10. Nakajo M, Shapiro B, Copp J, et al. The normal and abnormal distribution of adrenomedullary imaging m-(I-131)iodobenzylguanidine in man: evaluation by scintigraphy. *J Nucl Med* 1983;24:672–682.
11. Shapiro B, Copp JE, Sisson JC, et al. I-131-metaiodobenzylguanidine for the locating of suspected pheochromocyroma: experience in 400 cases. *J Nucl Med* 1985;26:576–585.
12. Tada M, Matsuzawa T, Ohrui H, et al. Synthesis of some 2-deoxy-2-fluoro-[^{18}F]hexopyranoses: potential diagnostic imaging agents. *Heterocycles* 1984;22:565–568.
13. Fukuda H, Matsuzawa T, Tada M, et al. 2-Deoxy-2-[^{18}F]fluoro-D-galactose: a new tracer for the measurement of galactose metabolism in the liver by positron emission tomography. *Eur J Nucl Med* 1986;11:444–448.
14. Yamaguchi K, Matsuzawa T, Fukuda H, et al. New liver functional imaging using 2-deoxy-2-(F-18)-fluoro-D-galactose (F-18) FDGal. *CYRIC Annual Report (Tohoku University)* 1986;1985:205–211.
15. Tada M, Matsuzawa T, Yamaguchi K, Abe Y, Fukuda H, Itoh M. Synthesis of ^{18}F-labeled 2-deoxy-2-fluoro-D-galactopyranoses using acetyl hypofluorite procedure. *Carbohydr Res* 1987;161:314–317.
16. Fukuda H, Yamaguchi K, Matsuzawa T, et al. 2-deoxy-2-[^{18}F]fluoro-D-galactose: a new tracer for the evaluation of liver function by PET. I. Evaluation of toxicity and radiation dose. *Jpn J Nucl Med* 1987;24:165–169.
17. Fukuda H, Yamaguchi K, Matsuzawa T, et al. 2-deoxy-2-[^{18}F] fluoro-D-galactose: a new probe for the evaluation of liver function by PET. II. A first clinical PET study of the liver in normal volunteers. *Jpn J Nucl Med* 1987;24:871–874.
18. Ishiwata K, Ido T, Imahori Y, Yamaguchi K, Fukuda H, Matsuzawa T. Accumulation of 2-deoxy-2-[^{18}F] fluoro-D-galactose in the liver by phosphate and uridylate trapping. *Nucl Med Biol* 1988;15:271–276.
19. Ishiwata K, Yamaguchi K, Kameyama M, et al. 2-Deoxy-2-[^{18}F]fluoro-D-galactose as an in vivo tracer for imaging galactose metabolism in tumors with positron emission tomography. *Nucl Med Biol* 1989;16:247–254.
20. Fukuda H, Yamaguchi K, Matsuzawa T, et al. Imaging of hepatocellular carcinoma with 2-deoxy-2-[^{18}F]fluoro-D-galactose by PET [Abstract]. *J Nucl Med* 1987;28:706.
21. Fukuda H, Yamaguchi K, Matsuzawa T, et al. Imaging of hepatoma with ^{18}F-deoxyfluorogalactose using PET. *Tumor Diagnostik & Therapie* 1988; 9:171.
22. Fujiwara T, Kubota K, Sato T, et al. N-[^{18}F]fluoroacetyl-D-glucosamine: a potential agent for cancer diagnosis. *J Nucl Med* 1990;31:1654–1658.
23. Sato H, Belkin M, Essner E. Experiments on an ascites hepatoma. III. The conversion of mouse hepatomas into the ascites form. *J Natl Cancer Inst* 1956;17:1–21.
24. Shatton JB, Morris HP, Weinhouse S. Kinetic, electrophoretic, and chromatographic studies on glucose-ATP phosphotransferase in rat hepatomas. *Cancer Res* 1969;29:1161–1172.
25. Ono T. Enzyme patterns and malignancy of experimental hepatomas. In: Yoshida T, Yashida T, eds. *Biological and biochemical evaluation of malignancy in experimental hepatomas. Gann monograph on cancer research volume 1.* Tokyo: Japanese Cancer Association; 1966:189–205.
26. Yoshida T, Odashima S, Kurata T, et al. Studies on the ascites hepatoma (XII). Report on establishment of nine further transplant strains. *Jpn J Cancer Res (Gann)* 1957;48:551–552.
27. Cuatrecasas P, Segal S. Mammalian galactokinase. Development and adaptive characteristics in the rat liver. *J Biol Chem* 1965;240:2383–2388.
28. Tygstrup N. Determination of the hepatic galactose elimination capacity after a single intravenous injection in man: the reproducibility and the influence of uneven distribution. *Acta Physiol Scand* 1963;58:162–172.
29. Tygstrup N. The galactose elimination capacity in control subjects and in patients with cirrhosis of the liver. *Acta Med Scand* 1964;175:281–289.
30. Bauer CH, Buchsel R, Morris HP, Reutter WG. Alteration of D-galactose metabolism in Morris hepatomas. *Cancer Res* 1980;40:2026–2032.
31. Abe Y, Fukuda H, Yamada K, et al. Studies on (F-18)-labeled pyrimidines: tumor uptake of (F-18)-5-fluorouracil, (F-18)-fluorouridine and (F-18)-fluorodeoxyuridine in animal studies. *Eur J Nucl Med* 1983;8:258–261.
32. Kubota K, Yamada K, Fukuda H, et al. Tumor detection with carbon-11-labeled amino acids. *Eur J Nucl Med* 1984;8:136–140.